Chemical Physics 172 (1993) 325–338
North-Holland

Spectroscopy of jet-cooled benzimidazole and benzotriazole

Erko Jalviste and Aleksei Treshchalov
Institute of Physics, Estonian Academy of Sciences, Riia 142, EE2400, Tartu, Estonia

Received 11 January 1993

Laser-induced fluorescence excitation and dispersed fluorescence spectra of jet-cooled benzimidazole and benzotriazole molecules are reported. The first excited singlet state is assigned to ^1L_b for benzimidazole (origin at 36032 cm^{-1}) and to ^1L_a for benzotriazole (origin at 34927 cm^{-1}). A rapid nonradiative decay is found to occur for benzotriazole above 1200 cm^{-1} from S_1 origin. The spectra of benzimidazole show a good Franck–Condon overlap between S_0 and $S_1(^1L_b)$ states. For benzotriazole progressions of several in-plane modes (540, 1153, 1242, 1405 and 1447 cm^{-1}) cover about 8000 cm^{-1} of the dispersed fluorescence spectrum following excitation into the origin of the $S_1(^1L_a)$ state.

1. Introduction

The near-UV singlet–singlet absorption transitions of benzo-derivatives of five-membered heterocycles, including indole, benzimidazole and benzotriazole, are $\pi^*\leftarrow\pi$ type transitions to two excited electronic states, ^1L_a and ^1L_b. Both transitions are symmetry-allowed because of their in-plane transition dipole moments [1].

Among these molecules the most thoroughly studied molecule is indole. Its weaker ^1L_b transition with the oscillator strength $f=0.01$ has a dominant 0–0 band (origin) and short Franck–Condon progressions of a few modes but the ^1L_a ($f=0.07$) transition forms a broad band with a hardly noticeable vibrational structure in the absorption spectrum. The origins of the ^1L_a and ^1L_b states may lie close in energy, although the absorption maximum of the ^1L_a state lies 3000 cm^{-1} above the ^1L_b origin [1–3]. The ^1L_b origin of gas-phase indole is located at 35233 cm^{-1}. A large amount of recent experimental work has been devoted to find spectral and temporal manifestations of the near-lying ^1L_a state for jet-cooled indole, substituted indoles and their complexes with various solvents (see refs. [4–6] and references therein).

The room-temperature UV absorption, fluorescence, phosphorescence spectra and respective polarization spectra of benzimidazole and benzotriazole solutions with various solvents have been measured and analysed in ref. [1]. Benzimidazole shows a structured ^1L_b band and a broad ^1L_a band whose origin lies about 4000 cm^{-1} higher than the ^1L_b origin. For benzotriazole the opposite ordening of ^1L_a and ^1L_b states has been found: the ^1L_a origin lies about 4000 cm^{-1} lower than that of the ^1L_b state. Both absorption bands are broad and smooth; however, the fluorescence coming from the ^1L_a state exhibits a clearly visible vibrational structure [1]. Vibrational analysis and rotational contour analysis of the 0–0 band of the vapour-phase benzimidazole $S_1\leftarrow S_0$ absorption spectrum have been reported in refs. [7] and [8], respectively. The data concerning the ground state vibrations derived from Raman and IR spectra have been summarized in ref. [9] for benzimidazole and in ref. [10] for benzotriazole.

An important peculiarity of benzimidazole and benzotriazole is proton tautomerism [11]. Both molecules have two identical tautomers (1H and 3H); benzotriazole can form, in principle, also 2H-tautomer (fig. 1). However, experimentally only 1H-tau-

Fig. 1. Tautomers of benzotriazole: 1H-tautomer with C_s symmetry and 2H-tautomer with C_{2v} symmetry.

tomer of benzotriazole has been observed in the crystalline phase [12] as well as in the solution [11]. The problem is analogous in the case of the 1,2,3-triazole molecule, where only 2H-tautomers are observable in the gas phase, while in solution both tautomers have been found [13].

The present work is aimed to obtain spectroscopic information about isolated benzimidazole and benzotriazole molecules, especially about the proton tunnelling or transfer effects in excited states. This paper includes also the results of our previous work about benzotriazole [14], the spectra being recorded once more with a better resolution. The influence of mode-mixing effects and the nature of the first excited state (^1L_a versus ^1L_b) on the observed excitation and single-vibronic-level dispersed fluorescence spectra will be discussed.

2. Experimental

The powder of benzimidazole (benzotriazole) was heated to 140°C (160°C); the mixture of the sample vapour with the Ar carrier gas (typical pressure 20 kPa) was continuously expanded into vacuum through a 0.2 mm orifice. The vacuum of 0.2 Pa was maintained with a 700 ℓ/s booster pump NVBM-0.5 backed by a 5 ℓ/s rotary pump 2NVR-5D. No differences have been found in the excitation spectra after twofold recrystallization of samples from ethanol; therefore commercially available chemicals without additional purification were used, afterwards.

The fluorescence was excited with a frequency-doubled dye laser VL-22, pumped by an ELI-73 excimer laser at a repetition rate of 5 Hz. A frequency-doubled unfocused dye laser beam (diameter 1 mm, fwhm 0.4 cm^{-1}, pulse energy 40 μJ) crossed the jet 5 mm downstream the nozzle. The excitation spectra were obtained by measuring the total undispersed emission; the dispersed fluorescence spectra were measured by one half of a DFS-24 0.82 m double monochromator in the second order of the 1200 grooves/mm grating. In both cases the signal was detected by a UV photomultiplier FEU-106, processed by a boxcar-integrator BCI-280 and recorded with a chart-recorder.

The excitation spectra were not normalized to laser intensity. In these spectra the strong bands may have been partly affected by saturation effects. The dispersed fluorescence spectra were normalized to the total fluorescence signal. Some of the fluorescence spectra are quite noisy due to photon statistics of a weak signal. No cut-off filters were used to discriminate against the scattered laser radiation. For the resonance fluorescence signal the amount of scattering was found to be negligible for the 0–0 band of benzimidazole and about 20% for the 0–0 band of benzotriazole. However, for weaker bands the contribution from scattering may be considerably larger.

3. Results

3.1. Benzimidazole

Fig. 2 shows the $S_1 \leftarrow S_0$ fluorescence excitation spectrum of benzimidazole. The data obtained from this spectrum are presented in table 1. Some hot sequence bands (with intervals 11, 52, 63 and 138 cm^{-1}) appear towards the red of a very strong 0–0 band at 36032 cm^{-1}, because of insufficient cooling in our continuous Ar jet. In the absorption spectrum of benzimidazole vapour [7] the strong sequences emerge from these bands. The hot bands are assigned to the $1 \leftarrow 1$ vibronic transitions of low-frequency out-of-plane modes. The pattern of hot bands is well repeated for the fundamentals up to 729 cm^{-1}. For hot bands associated with higher frequency fundamentals the intervals (particularly the 11 cm^{-1} one) are perturbed by mode-mixing effects.

Fig. 3 shows a dispersed fluorescence spectrum following excitation into the 0–0 band. The ground state vibrational frequencies up to 1700 cm^{-1} determined from this spectrum and correlated with those from infrared, Raman and solid state fluorescence data from ref. [9] are summarized in table 2. The similarity of band intensities in our 0–0 band fluorescence spectrum and in that of solid benzimidazole from ref. [9] helped us greatly to correlate the bands; however, some uncertainties remain. The 1079 cm^{-1} band is tentatively correlated with the 1138 cm^{-1} NH in-plane bending mode observed in crystalline benzimidazole. A large frequency shift can be explained by hydrogen bonding in the solid phase. The band at 1395 cm^{-1} is too strong to be attributed to the 776+620 cm^{-1} combination band only; therefore,

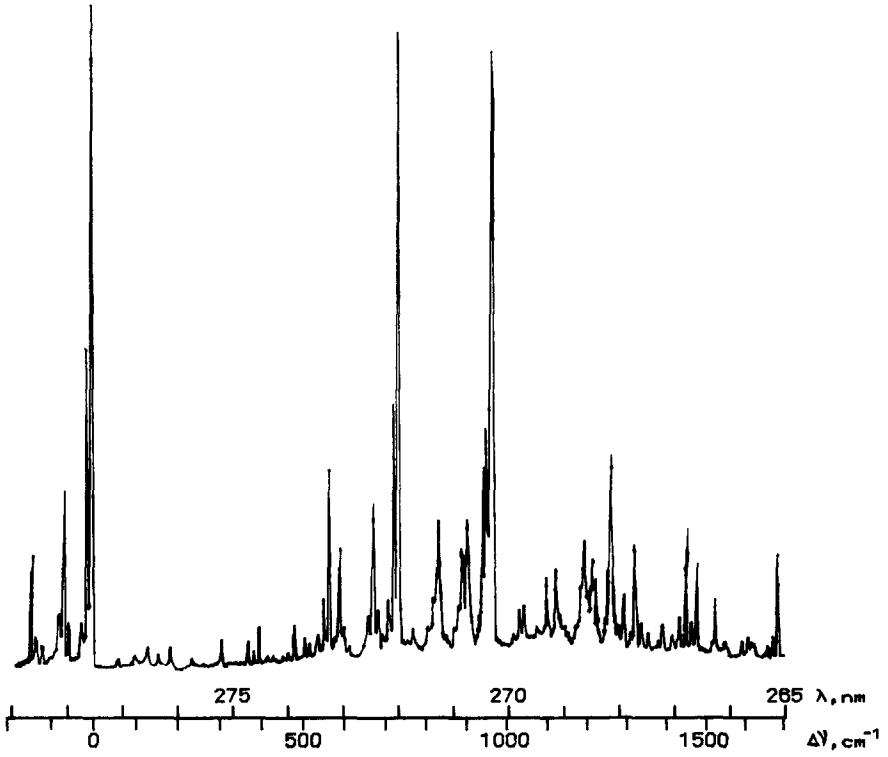

Fig. 2. Fluorescence excitation spectrum of benzimidazole. The zero for Δv corresponds to the 0–0 band.

this band may correspond to the 1412 cm^{-1} fundamental in the fluorescence spectrum of the solid. Some weak bands at 433, 852 and 1424 cm^{-1} are correlated to IR and Raman bands for which out-of-plane symmetry was established. Their existence can be explained in terms of the Hertzberg–Teller coupling. The out-of-plane symmetry of the strong 1360 cm^{-1} band is still doubtful. For shortness only the assignments of a few stronger combination bands are included in table 2, though most of these bands are assigned. The frequencies of the ground and the excited state fundamentals agree well with the ones determined from the vapour-phase absorption spectrum [7]. However, in the vapour-phase spectrum the 36023 cm^{-1} feature, which is assigned to the 0–0 band in refs. [7,8], may actually be a sequence band.

In order to find a correspondence between the excited and the ground state modes the fluorescence spectra of the strongest excited state fundamentals were recorded. In the case of a good overlap between the excited and the ground state wavefunctions the strongest feature in the dispersed fluorescence spectra following excitation into the upper state vibronic levels is the band corresponding to the $\Delta v=0$ ($1\rightarrow1$) vibronic transition, which serves as the origin for the other bands forming a spectrum resembling the one resulting from 0–0 excitation. The distance between the $\Delta v=-1$ (resonance fluorescence) and the $\Delta v=0$ bands is the frequency of the ground state mode sought for (see refs. [15,16]). The ground state counterparts of the excited state modes up to 729 cm^{-1} determined in this way are given in table 3. The 433, 467 and 635 cm^{-1} modes in the fluorescence spectrum following excitation into the 0–0+303 cm^{-1} band, are probably out-of-plane modes mixed with one another by the Dushinsky effect.

Excitation into the hot sequence bands associated with the 0–0 band yields spectra similar to the 0–0 band dispersed fluorescence but shifted to an apparent origin (the resonance band) due to the difference in out-of-plane mode frequencies for S_0 and S_1. Only for the -138 cm^{-1} hot band a very weak extra band

Table 1
Assignments of the excitation spectrum of benzimidazole. Accuracy is ±2 cm^{-1}. Hot bands are marked by h, fundamentals by f and uncertain assignments by ?

$\Delta\nu$ (cm^{-1})	I	Assignment	$\Delta\nu$ (cm^{-1})	I	Assignment
−138	m	h	1032	w	(729+303) ?
−76	w	h, −63−11	1041	w	
−63	m	h	1092	m	
−52	w	h	1123	m	(729+396) ?
−23	w	h, −2*11	1133	vw	
−11	s	h	1173	vw	
0	vs	origin	1190	m	
158	vw	f	1193	m	
188	vw	f	1216	m	
237	vw		1221	m	
303	w	f	1257	s	
369	w	f	1262	s	f
384	vw	h, 396−11	1276	vw	
396	w	f	1291	w	(729+566)
414	vw	h, 477−63	1310	vw	
462	vw	h, 477−11	1321	m	f
477	w	f	1339	w	
501	vw	h, 566−63	1343	w	
514	vw	h, 566−52	1361	vw	(960+396) ?
538	vw		1381	vw	
555	w	h, 566−11	1395	w	
566	s	f	1420	vw	
593	m	h, 729−138	1437	vw	(960+477) ?
651	w	h, 729−63−11	1449	w	
665	m	h, 729−63	1459	m	2*729
677	w	h, 729−52	1469	w	
700	w	h, 729−2*11	1480	m	
715	s	h, 729−11	1531	w	(960+566)
729	vs	f	1556	vw	
767	vw		1562	vw	
828	m	f	1611	vw	
884	m	f	1624	vw	
895	m	h, 960−63	1661	vw	
923	vw		1676	vw	
936	s	f	1691	m	(960+729)
944	s	h, 960−11	1700	vw	
960	vs	f			
964	s				

in fluorescence, shifted by 210 cm^{-1} to the blue from the resonance band, was detected.

Excitation into the bands higher than 800 cm^{-1} above the 0–0 band produced a pattern of bands in the $\Delta v=0$ region in emission, whose complexity increases with the excitation energy. The frequency intervals and the relative intensities for stronger bands in the $\Delta v=0$ region are listed in table 3. Figs. 4, 5 and 6 show the fluorescence spectra following excitation into the 960, 964 and 2*729 cm^{-1} bands above the S_1 origin, respectively.

The complexity of the fluorescence patterns in the $\Delta v=0$ region of spectra, which increases together with the density of vibrational states, indicates that the fluorescence comes from the level (or a number of overlapped levels) representing a superposition of several zero-order vibrational states coupled via anharmonicities (e.g. showing a Fermi resonance) or

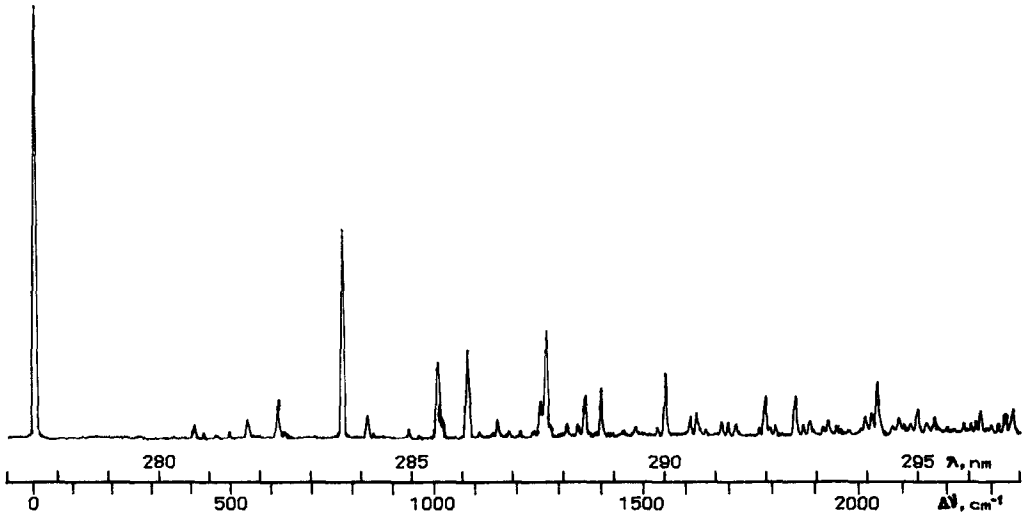

Fig. 3. Dispersed fluorescence spectrum of benzimidazole excited into the 0–0 band. Resolution 0.045 nm (6 cm^{-1}). The zero for $\Delta\nu$ corresponds to resonance fluorescence; $\Delta\nu > 0$ indicates red-shifts.

otherways. The zero-order modes mixed by couplings are classified to optically inactive (dark) modes, for which only the $\Delta v = 0$ transitions are allowed, and active (bright) ones, for which also the $\Delta v \neq 0$ transitions are allowed [15]. Hence the active modes carry the oscillator strength from the ground state 0-level. The intensity redistribution to inactive modes gives rise to strong bands in the $\Delta v = 0$ region (for example the 1030, 1066 and 1300 cm^{-1} bands) of fluorescence spectra following excitation into the bands 800 cm^{-1} above the origin, although the bands with the same frequencies are absent or very weak in the fluorescence spectrum excited to the 0–0 band. The mode-mixing, which finally turns into IVR (intramolecular vibrational redistribution) at high vibrational energies, is a well known effect which for some large organic molecules has been investigated in detail [15,17,18]. Mode-mixing and the lack of mirror symmetry of benzimidazole spectra does not allow to establish the correspondence between the excited and the ground state modes, whose frequencies exceed 800 cm^{-1}.

Among the upper state Fermi-resonance pairs, 960; 964 cm^{-1} (see fluorescence spectra in figs. 4 and 5) and 1257; 1262 cm^{-1}, the 0–0+960 and 0–0+1262 cm^{-1} bands seem to be of mostly optically active zero-order character. The fluorescence spectra following excitation into the "inactive" bands, 0–0+964 and 0–0+1257 cm^{-1}, contain a group of bands with similar frequency intervals and intensity distribution: the 1030, 1315, 1344 cm^{-1} and the 1300, 1590, 1622 cm^{-1} bands, respectively (see table 3). For an explanation it is assumed that the combination modes, acting as emitting states, include one or more common fundamentals.

The 776; 729 cm^{-1} (ν''; ν') breathing mode forms a progression both in excitation and fluorescence spectra (see figs. 2, 3 and 6). This refers to the expanded excited state configuration of benzimidazole. A Franck–Condon analysis (table 4) using a displaced harmonic oscillator model [19], yielded for the distortion parameter γ of this mode the value of 0.7. The Franck–Condon factors are expressed in terms of two parameters γ and $\beta = (\nu''/\nu')^{1/2}$, the parameter γ being related to the displacement d along a normal coordinate, $\gamma = -(4\pi^2\nu'/h)^{1/2} d\beta/(1+\beta^2)^{1/2}$ as in ref. [20]. If anharmonic couplings between the modes are neglected (zero-order case), the fluorescence from excitation into the 0–0+729 cm^{-1} (or 0–0+2*729 cm^{-1}) bands ought to consist of dispersed superimposed spectra, each similar to that observed for a 0–0 excitation but belonging to transitions which start from one (or two) quanta in the breathing mode of S_1 and end in levels of S_0 with up to four breathing quanta combined with excitation of all other active S_0-modes. For the 0–0+729

Table 2
Frequency shifts of the bands of the dispersed origin fluorescence spectrum of jet-cooled benzimidazole together with the Raman, infrared and fluorescence data of solid benzimidazole, and symmetry assignments for fundamentals from ref. [9]. The relative intensity, I, is shown for the jet and the solid state fluorescence data

Jet fluorescence		IR	Raman	Solid fluorescence		Assignment
$\Delta\nu$ (cm^{-1})	I	ν (cm^{-1})	$\Delta\nu$ (cm^{-1})	$\Delta\nu$ (cm^{-1})	I	
0	400					
414	6	419		419	1	a′
433	5	424	422			a″
467	1					
502	7					
543	17	544	547	542	7	a′
620	36	619	620	617	16	a′
776	190	772	780	777	86	a′
839	21	837				
852	8	848	851	849	3	a″
869	5					
939	10	950	962	963	2	a′
1009	82	1006	1008	1003	34	a′
1021	15					
1052	2					
1079	75	1138	1139	1138	35	a′
1115	2	1115	1112			a′
1154	18	1155	1160	1159	5	a′
1183	4	1185	1191	1193	4	a′
1207	6	1200	1206			a′
1240	8					2*620
1254	46	1250	1251			a′
1268	102	1263	1277	1277	100	a′
1297	2	1295	1306			a′
1318	13					(776+543)
1344	8		1349			a′
1360	38	1360	1368	1365	6	a″
1395	44	1410	1414	1412	13	a′ and (776+620)
1429	3		1421			a″
1458	8	1460	1463			a′
1482	7	1485	1481			a′
1498	4		1500			a′
1535	4					
1552	45			1549	11	2*776
1612	10					(776+840)
1631	18	1620	1623	1621	9	a′ and (1009+620)
1699	10					(1079+620)
1785	34					(1009+776)
1852	33					(1079+776)
2043	42					(1268+776)
2277	22					(1268+1009)
2347	28					(1268+1079)

cm^{-1} band this is actually the case, only the 776+1145 cm^{-1} combination band being anomalously strong. However, the dispersed fluorescence spectrum of the 0–0+2*729 cm^{-1} band (fig. 6) contains in addition to the zero-order band pattern other bands due to mode mixing (the strongest are the 1154,

Table 3
Correspondence between the S_1 and the S_0 state mode frequencies (in cm^{-1}) of benzimidazole. In case that more than one band appeared in the $\Delta v=0$ region of the fluorescence spectrum, the frequency shifts (in cm^{-1}) and percent fractions of relative intensities for all strong $\Delta v=0$ bands are presented

Excited state	Ground state
158	≈210
188	≈220
303	433(70), 467(15), 635(15)
369	502
396	414
477	543
566	620
729	776
828	869(39), 1052(26), 1168(20), 1254(7), 1344(8)
936	1009(10), 1066(80), 1207(10)
960	1030(23), 1071(7), 1079(18), 1115(6), 1254(9), 1268(7), 1275(10), 1315(12), 1344(8)
964	1030(33), 1079(6), 1315(15), 1344(19), 1413(13), 1498(8), 1648(6)
1257	1268(11), 1300(39), 1498(5), 1520(5), 1590(12), 1622(12), 1704(16)
1262	1262(8), 1300(17), 1424(7), 1463(8), 1498(15), 1520(9), 1565(9), 1590(11), 1622(8), 1743(8)
1321	1079(7), 1318(7), 1360(11), 1395(25), 1498(6), 1539(6), 1597(7), 1616(6), 1699(13), 1793(4), 1810(8)

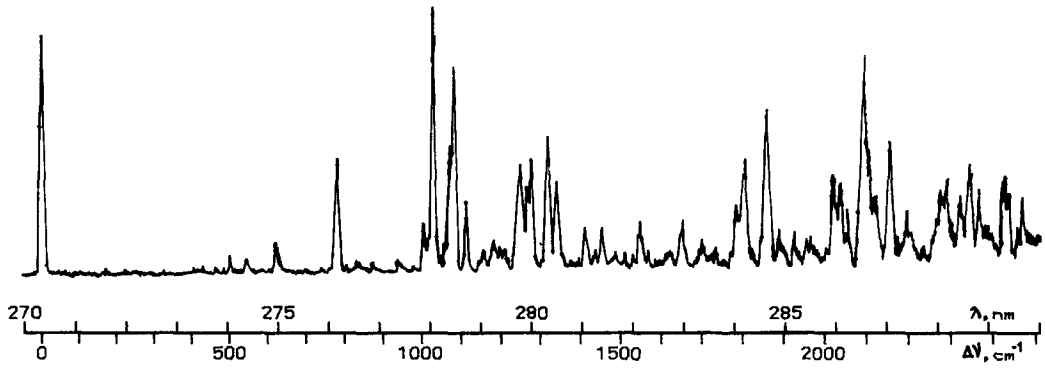

Fig. 4. Dispersed fluorescence spectrum of benzimidazole excited into the 0–0+960 cm^{-1} band (the "bright" component of the 960; 964 cm^{-1} Fermi-resonance doublet of S_1). Resolution 0.068 nm (9 cm^{-1}).

776+1009 and 2*1009 cm^{-1} bands) and an almost continuous background located to the red from 278.5 nm. Due to anharmonic couplings the 2*776+1079 and 2*776+1154 cm^{-1} combination bands are relatively strong although the 2*776 cm^{-1} band is very weak. The appearance of the continuous background indicates that IVR begins to have effect at 1450 cm^{-1} above the S_1 origin.

3.2. Benzotriazole

Fig. 7 shows the $S_1 \leftarrow S_0$ fluorescence excitation spectrum of jet-cooled benzotriazole. The observed bands are listed in table 5. All the bands located to the red from the strong 0–0 band (34927 cm^{-1}) are attributed to hot sequence bands, because their intensity relative to that of the 0–0 band decreases when

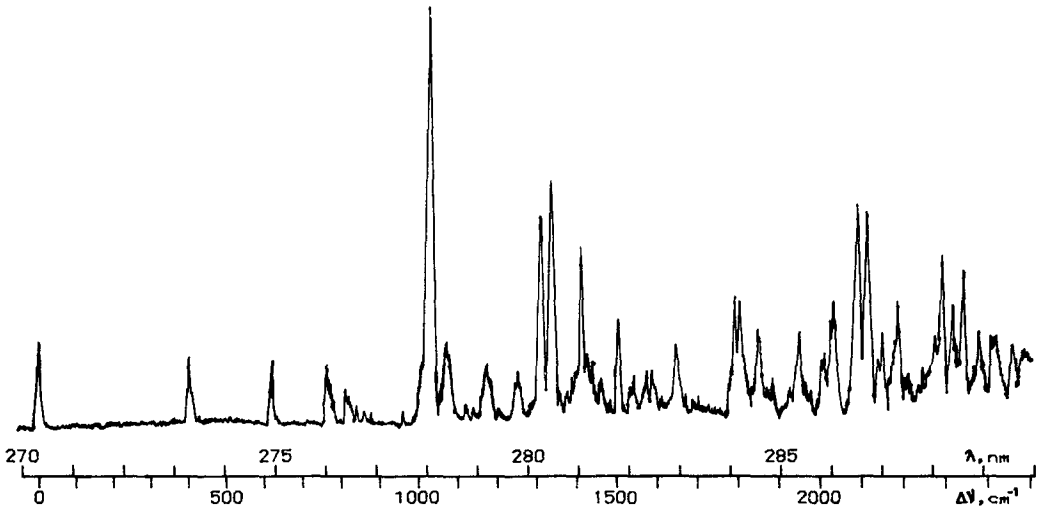

Fig. 5. Dispersed fluorescence spectrum of benzimidazole excited into the 0–0+964 cm^{-1} band (the "dark" component of the 960; 964 cm^{-1} Fermi-resonance doublet of S_1). Resolution 0.09 nm (12 cm^{-1}).

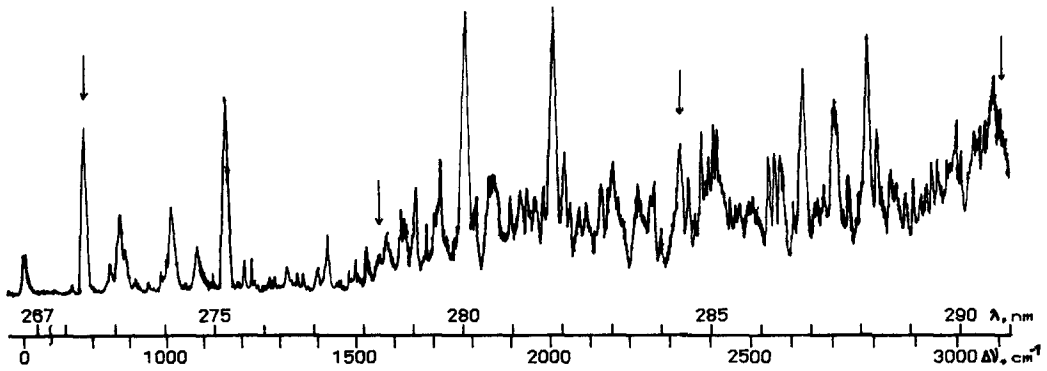

Fig. 6. Dispersed fluorescence spectrum of benzimidazole excited into the 0–0+2*729 cm^{-1} overtone band of the breathing mode. Resolution 0.14 nm (18 cm^{-1}). Members of the 776 cm^{-1} breathing mode progression in S_0 are indicated by arrows. Note the scale gap.

Ar pressure is raised. Two hot bands at -566 and -540 cm^{-1} from the origin are supposed to be $0 \leftarrow 1$ vibronic transitions originating from the 566 and the 540 cm^{-1} ground state modes, respectively. Some hot bands may represent the $1 \leftarrow 1$ transitions of out-of-plane modes.

A quick onset of the congestion of bands towards the blue in the exitation spectrum hints to strong anharmonicity of the upper state potential. Above 1200 cm^{-1} from the 0–0 band only a weak and broadened band, assigned to the 795+481 cm^{-1} combination band, appears due to a rapid intensity decline. This indicates effective coupling to some nonradiative manifold. The proceeding of the absorption towards the blue is clearly visible in the absorption spectrum of benzotriazole in solution [1].

The low-resolution dispersed fluorescence survey-spectrum of benzotriazole excited to the 0–0 band is presented in fig. 8. The same spectrum taken with a better resolution is shown in fig. 9. Its 90 nm extent and its intensity maximum lying in the centrum implies a large change in geometric configuration on the S_1–S_0 electronic excitation. The frequencies and assignments of the observed bands are shown in table

Table 4
Franck–Condon analysis of the 776; 729 cm^{-1} breathing mode of benzimidazole. Calculated squared FC factors for the distortion parameter $\gamma=0.7$ are compared with the observed relative intensities (in parentheses) of relevant bands in fluorescence spectra excited into 0–0, 0–0+729 and 0–0+2*729 cm^{-1} bands

v'	v''				
	0	1	2	3	4
0	0.61	0.29	0.08	0.02	
	(0.62)	(0.29)	(0.07)	(0.02)	
1	0.31	0.16	0.32	0.16	0.05
	(0.25)	(0.15)	(0.34)	(0.16)	(0.04)
2	0.07	0.37	0.01	0.24	0.20
	(0.08)	(0.33)	(0.03)	(0.24)	(0.29)

6. We had no success in correlating the observed fundamentals in our spectrum with the IR and Raman bands known from solution spectra [10], because of large discrepancies between the frequencies and intensities of the bands. Only the strong 540 cm^{-1} band seems to correspond to the Raman band of the same frequency. If this is indeed so, then the 540 cm^{-1} mode cannot be triazole ring torsion as assigned in ref. [10]; it must be an in-plane mode, provided that benzotriazole is planar in both S_0 and S_1 states. The 783 cm^{-1} breathing mode, which forms a strong band in the Raman and the IR spectra, does not appear in our 0–0 band fluorescence spectrum. Also, the lack of the 566 cm^{-1} band is surprising, because in the excitation spectrum there exist both the -540 and the -566 cm^{-1} hot bands.

An analysis of the higher-frequency part of the 0–0 band dispersed fluorescence spectrum (table 6) revealed that it is dominated by the combination bands of strong 540, 1153, 1242, 1405, and 1447 cm^{-1} fundamentals. A comparison of the 0–0 band fluorescence spectra in figs. 8 and 9 reveals that the strong features in the low-resolution spectrum are formed by a number of bands coinciding within the spectral resolution of the monochromator, while the intensity of some single band is generally weaker than that of resonance fluorescence. The intensity maximum lies in the region where three vibrational quanta of 1153, 1242, 1405, and 1447 cm^{-1} modes combine. The third overtones of these vibrations are already very weak compared to the combination bands. This means that on electronic transition the geometric configuration of benzotriazole shifts along several normal coordinates, but not along the coordinate of a single mode as stated in our previous work [14]. We tried to simulate the 0–0 band fluorescence spectrum in the framework of an independent (parallel) harmonic oscillator model [21]. The intensities (squared Franck–Condon factors) of the fundamentals and the overtones of each mode were taken proportional to $\gamma^{2v}/v!$, where γ is the distortion parameter and v is the number of quanta for the corresponding mode. The intensities of combination modes were calculated as products of the intensities of fundamentals from which they are made up. A

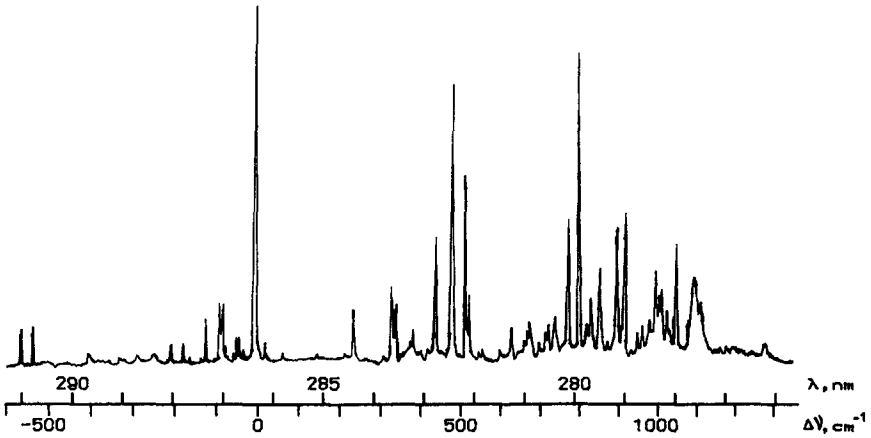

Fig. 7. Fluorescence excitation spectrum of benzotriazole.

Table 5
Assignments of the fluorescence excitation spectrum of benzotriazole. Accuracy ± 2 cm^{-1}

$\Delta\nu$ (cm^{-1})	I	Assignment	$\Delta\nu$ (cm^{-1})	I	Assignment
−566	m	h	663	w	
−540	m	h	679	w	
−210	w	h	716	vw	
−183	w	h	721	w	
−127	m	h, −566+439	740	w	
−93	m	h	774	s	
−86	m	h, −566+481	795	vs	
−59	w	h, −566+510	828	w	
−49	w	h, −566+519	851	m	
0	vs	origin	894	s	
24	w	h	914	s	
67	vw	h, −566+633	947	vw	
238	m		959	w	2*481
331	m		974	w	
339	m		988	m	(510+481)
374	w		998	m	(519+481)
381	w		1006	m	
439	s		1018	w	2*510
481	vs		1045	s	
510	s		1089	m	
519	m		1094	m	
633	w		1102	m	
655	vw		1108	m	
			1274	vw	(795+481)

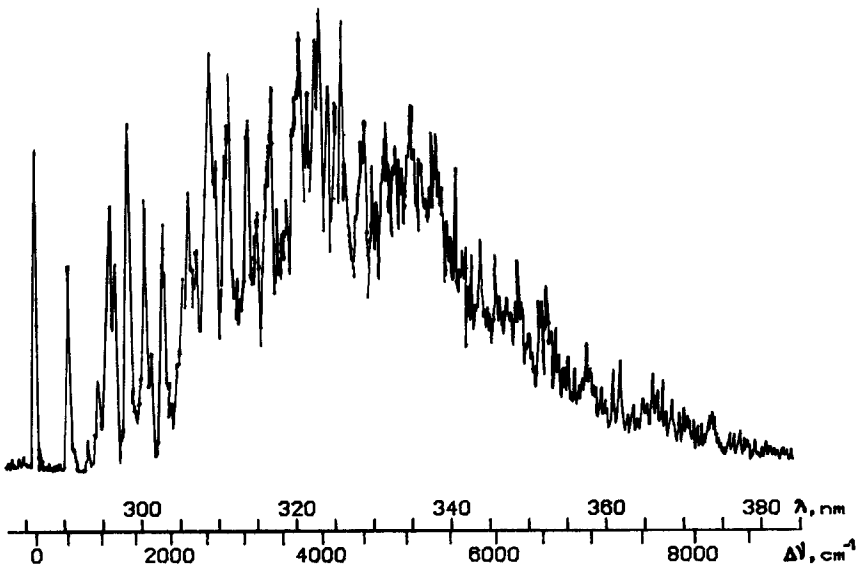

Fig. 8. Dispersed fluorescence spectrum of benzotriazole excited into the 0–0 band. Low resolution, 0.45 nm (43 cm^{-1}).

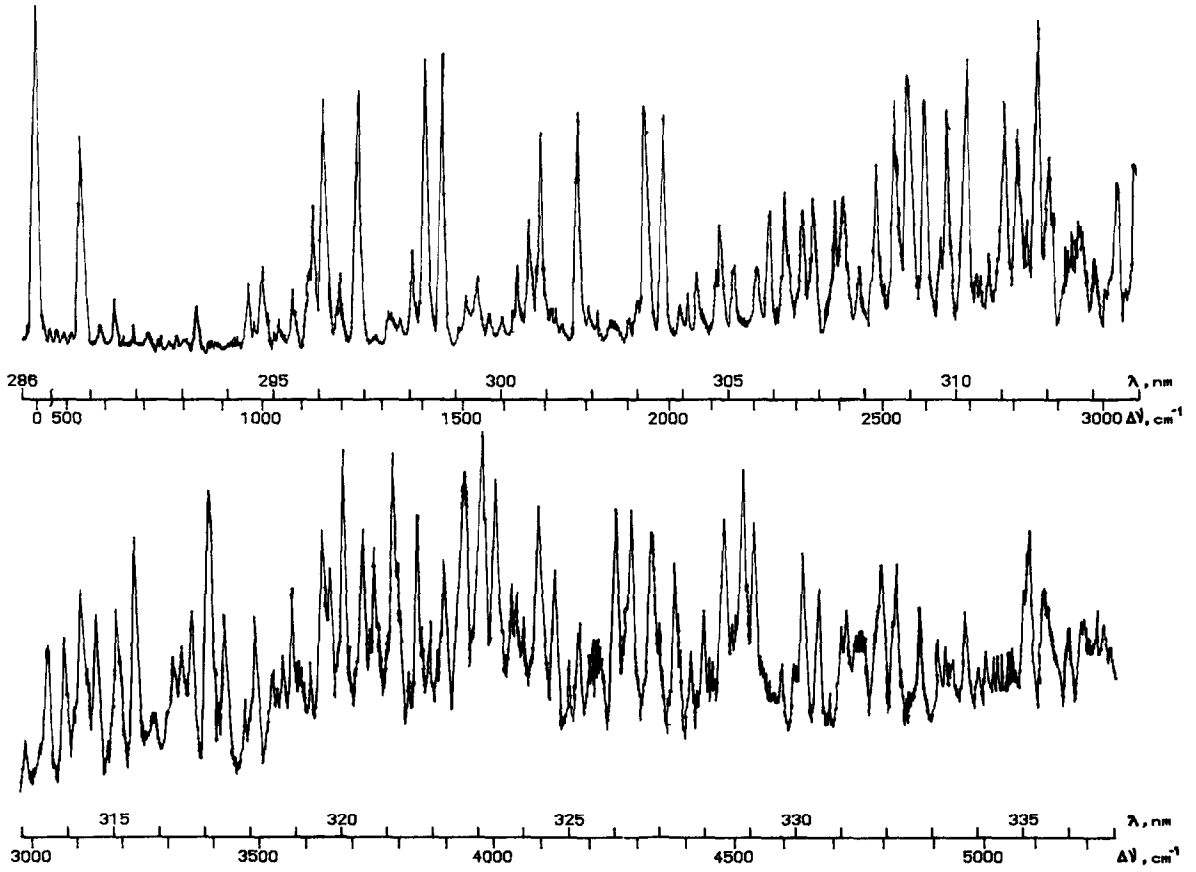

Fig. 9. Dispersed fluorescence spectrum of benzotriazole excited into the 0–0 band. High resolution, 0.14 nm (13 cm^{-1}). Note the scale gap.

qualitative resemblance with the experimental spectrum was obtained with the set of distortion parameters 0.85, 0.95, 0.95, 1.0 and 1.0 for 540, 1153, 1242, 1405 and 1447 cm^{-1} modes, respectively. We did not go on with a more refined modelling because the measured intensities of the bands are poorly reproducible due to weak signal strength.

In the third column of table 6 the frequency differences of combination modes in the pairs made up by combining the 1405 and 1447 cm^{-1} fundamentals with the same set of other modes are listed. These intervals are well reproduced also between the respective combinations with the 540 cm^{-1} mode. Variation of these intervals is explained by anharmonic coupling effects (Fermi resonances). It should be noted that only static couplings can influence the fluorescence spectrum resulting from 0–0 excitation.

The dispersed fluorescence spectrum following excitation into the 0–0 + 481 cm^{-1} band is shown in fig. 10. The frequencies of some features determined from this spectrum are listed in table 7. Unlike for the 0–0 spectrum the 540 cm^{-1} band is weak but there exists a long progression (up to $v=4$) of the 540 cm^{-1} mode built on the 1320 cm^{-1} band. Two progressions of the 540 cm^{-1} mode are marked in fig. 10. Mode-mixing by the Dushinsky effect may be responsible for such a modification of the spectrum: the formation of a long single-mode progression at certain mixing parameters has theoretically been predicted in ref. [22]. Thus, we cannot state firmly that the 481 cm^{-1} mode is the upper state counterpart of the 540 cm^{-1} mode.

Table 6
Assignments of the dispersed origin fluorescence spectrum of benzotriazole. The intervals $\delta\nu$ between successive combination bands involving 1405 and 1447 cm^{-1} mode are listed to demonstrate the influence of anharmonicity

$\Delta\nu$ (cm^{-1})	I	Assignment	$\delta\nu$ (cm^{-1})	$\Delta\nu$ (cm^{-1})	I	Assignment	$\delta\nu$ (cm^{-1})
0	vs			2484	m	2*1242	
540	s	f		2528	s	(1405+1127)	32
590	vw	f		2560	s	(1447+1127)	
626	w	f				(1405+1153)	33
836	vw	f		2599	s	(1447+1153)	
963	w	f		2646	s	(1405+1242)	42
998	w	f		2688	s	(1447+1242)	
1078	w	2*540		2778	s	(2235+540)	
1127	m	f		2807	s	2*1405	41
1153	s	f		2848	vs	(1447+1405)	36
1192	w	f		2884	m	2*1447	
1242	s	f		2982	w	(2444+540)	
1374	w	f			...		
1405	vs	f	42	3429	m	(2884+540)	
1447	vs	f		3488	m		
1511	w	(963+540)		3572	m		
1536	w	(998+540)		3641	s	(2*1242+1153)	
1633	w			3685	vs	(1405+1153+1127)	
1664	m	(1127+540)		3719	s	(1405+2*1153)	34
1691	s	(1153+540)		3753	s	(1447+2*1153)	
1727	vw	(1192+540)		3792	vs	(1405+1242+1153)	48
1779	s	(1242+540)		3840	s	(1447+1242+1153)	
1943	s	(1405+450)		3898	m	(1405+2*1242)	34
1984	s	(1447+540)		3932	vs	(1447+2*1242)	
2066	w			3970	vs	(2*1405+1153)	29
2122	m			3999	vs	(1447+1405+1153)	
2205	w	(1242+963)		4094	s	(1447+1405+1242)	33
2235	m	(1242+998)		4128	m	(2*1447+1241)	
2272	m			4255	s	(1447+2*1405)	33
2315	m	2*1153		4288	s	(2*1147+1405)	
2336	m			4331	s	(3792+540)	
2389	m	(1242+1153)			...		
2410	m			4828	m	(4288+540)	
2444	w			5083	s	(3932+1153)?	
				5129	m	(3970+1153)?	

4. Discussion

The first excited state of benzimidazole is assigned to ^1L_b and that of benzotriazole to ^1L_a based on solvent shifts and fluorescence polarization measurements of the corresponding solutions [1]. We retain the same assignments for isolated molecules. Short progressions and a very strong 0–0 band in the excitation spectrum and fluorescence spectrum from the S_1 origin in the case of benzimidazole point to a good Franck–Condon overlap between S_0 and $S_1(^1L_b)$ states. Only the breathing mode forms a somewhat longer progression. On the contrary the overlap of S_0 with the $S_1(^1L_a)$ state for benzotriazole is poor: an analysis of the fluorescence spectrum following excitation into the 0–0 band indicates that the ground-state equilibrium configuration differs strongly from that of the excited state along the normal coordinates of several modes.

The geometric configuration and atomic masses of benzimidazole, benzotriazole and also indole are quite similar; therefore, close vibrational frequencies are expected to be observed in the spectra of these molecules. A tentative correlation between some low-

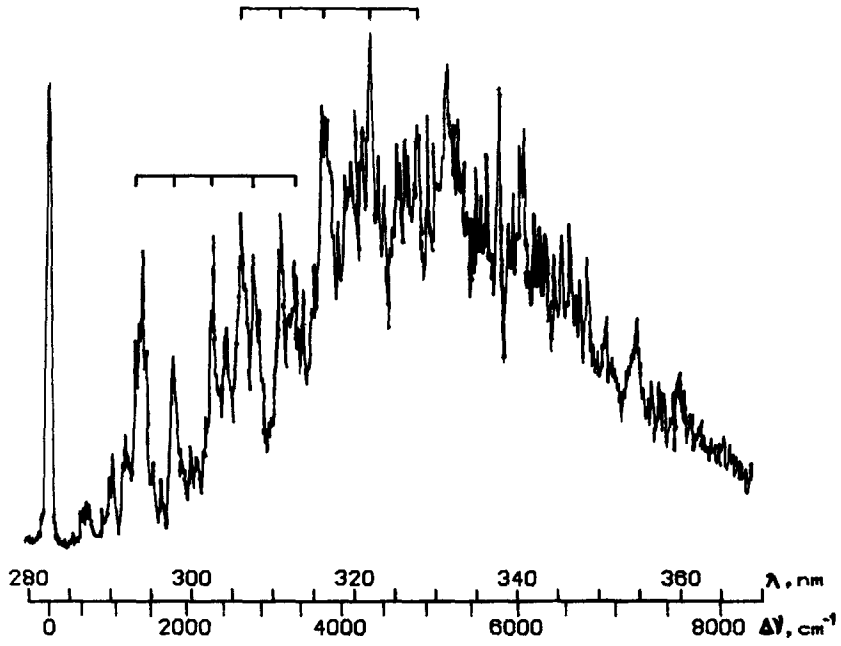

Fig. 10. Dispersed fluorescence spectrum of benzotriazole excited into the 0–0+481 cm^{-1} band. Resolution 0.54 nm (51 cm^{-1}). Two progressions of 540 cm^{-1} mode are indicated.

Table 7
Assignments of the strongest features in the dispersed fluorescence spectrum of benzotriazole excited to the 0–0+481 cm^{-1} band. Many features assigned to fundamentals are also observed in the origin fluorescence spectrum

$\Delta\nu$ (cm^{-1})	I	Assignment
0	s	
430	w	f
540	w	f, 540
670	w	f
980	m	f, 963 and f, 998
1160	m	f, 1153
1320	s	f
1420	s	f, 1405 and f, 1447
1860	m	(1320+540)
2400	s	(1320+2*540)
2760	vs	(1320+1420)
2840	vs	2*1420
2940	vs	(1320+3*540)
3300	vs	(1420+1320+540)
3490	vs	(1320+4*540)
3840	vs	(1420+1320+2*540)

frequency in-plane modes marked by a, b, c and d is established for these three molecules in table 8. In the excitation and 0–0 band fluorescence spectra of benzimidazole and indole b and c modes are intense, but in the spectra of benzotriazole a and d modes dominate. The prominence of particular modes in absorption and emission is related to certain changes of molecular geometry on electronic transition, which in turn depends on the excited state wavefunction (^1L_a or ^1L_b). Moreover, in a recent study two-photon excitation of jet-cooled indole with linearly and circularly polarized light permitted to distinguish the ^1L_a and ^1L_b type of vibronic bands [5]. It appeared that the vibronic bands of a and d modes exhibit ^1L_a character but that of b and c modes exhibit ^1L_b character. The ^1L_a or the ^1L_b character of bands is not reflected in their dispersed fluorescence spectra: the fluorescence spectra of indole [16] and benzimidazole following excitation into the a and b bands differ only with respect to the ground-state frequency. This can be explained if we assume that the strongest $1 \rightarrow 1$ band in fluorescence is induced by the same type of transition as one finds for the 0–0 band (^1L_b for indole and benzimidazole) although the relevant transition

Table 8
Frequency shifts (in cm^{-1}) and relative intensities of the bands belonging to the modes marked by a, b, c and d, in the excitation spectra (S_1 state data) and in the 0–0 band fluorescence spectra (S_0 state data) of indole, benzimidazole and benzotriazole: for benzotriazole ^1L_a-character modes (a and d) dominate, but for benzimidazole and indole ^1L_b-character modes (b and c) are more intense

Mode	Indole [a]		Benzimidazole		Benzotriazole	
	S_0	S_1	S_0	S_1	S_0	S_1
a	542(10)	480(35)	543(17)	477(10)	540(vs)	481(vs)
b	611(40)	540(42)	620(36)	566(45)	632(0) [b]	–
c	760(180)	718(175)	776(190)	729(175)	783(0) [b]	–
d	–	785(28)	–	–	–	795(vs)

[a] Data about indole are taken from ref. [16].
[b] Raman frequency taken from ref. [10].

in absorption (1←0 band) may be either of ^1L_a or ^1L_b type.

It is possible for benzotriazole that one of the two different tautomers (fig. 1) corresponds to the equilibrium configuration of the ground state while the other tautomer corresponds to that of the excited ^1L_a state. Briefly, proton transfer (tautomerization) accompanies the electronic transition. Proton transfer, dissociation by NH bond scission and/or the crossing of the ^1L_a and ^1L_b potentials may be responsible for the rapid termination of the excitation spectrum of benzotriazole above 1200 cm^{-1} from the ^1L_a origin. In the case of benzimidazole the barrier is probably too high to see spectral manifestations of proton tunneling.

References

[1] H.-U. Schütt and H. Zimmermann, Ber. Bunsenges. Physik. Chem. 67 (1963) 54.
[2] M.R. Eftink, L.A. Selvidge, P.R. Callis and A.A. Rehms, J. Phys. Chem. 94 (1990) 3469.
[3] E.H. Strickland and C. Billups, Biopolymers 12 (1989) 1973.
[4] D.R. Demmer, G.W. Leach, E.A. Outhouse, E.A. Hager and S.C. Wallace, J. Phys. Chem. 94 (1990) 582.
[5] D.M. Sammeth, S. Yan, L.H. Spangler and P.R. Callis, J. Phys. Chem. 94 (1990) 7340.
[6] M.J. Tinbergen and D.W. Levy, J. Phys. Chem. 95 (1991) 2175.
[7] R.D. Gordon and R.F. Yang, Can. J. Chem. 48 (1970) 1722.
[8] E. Cané, A. Trombetti, B. Velino and W. Caminati, J. Mol. Spectry. 150 (1991) 222.
[9] A. Suwaiyan, R. Zwarich and N. Baig, J. Raman Spectry. 21 (1990) 243.
[10] J. Rubim, I.G.R. Gutz, O. Sala and W.J. Orville-Thomas, J. Mol. Struct. 100 (1983) 571.
[11] J. Elguero, C. Marzin, A.R. Katritzky and P. Linda, The tautomerism of heterocycles (Academic Press, New York, 1976).
[12] A. Escande, J.L. Galigne and J. Lapasset, Acta Cryst. B 30 (1974) 1490.
[13] J.R. Cox, S. Woodcock, I.H. Hillier and M.A. Vincent, J. Phys. Chem. 94 (1990) 5499.
[14] E.H. Jalviste and A.B. Treshchalov, Proc. Estonian Acad. Sci. Phys. Math. 40 (1991) 213.
[15] P.M. Felker and A.H. Zewail, J. Chem. Phys. 82 (1985) 2961.
[16] Y. Nibu, H. Abe, N. Mikami and M. Ito, J. Phys. Chem. 87 (1983) 3898.
[17] S.M. Beck, J.B. Hopkins, D.E. Powers and R.E. Smalley, J. Chem. Phys. 74 (1981) 43.
[18] M. Fuji, T. Ebata, N. Mikami and M. Ito, Chem. Phys. 77 (1983) 191.
[19] J.B. Coon, R.E. DeWames and C.M. Loyd, J. Mol. Spectry. 8 (1962) 285.
[20] J.A. Syage, J.E. Pollard and J. Steadman, Chem. Phys. Letters 161 (1989) 103.
[21] M.D. Frank-Kamenetzky and A.V. Lukashin, Soviet Phys. Uspekhi 18 (1975) 391.
[22] H. Kupka and G. Olbrich, J. Chem. Phys. 82 (1985) 3975.